FLORE
Repository istituzionale dell'Università degli Studi di Firenze

Renal cells from spermatogonial germline stem cells protect against kidney injury

Questa è la Versione finale referata (Post print/Accepted manuscript) della seguente pubblicazione:

Original Citation:

Renal cells from spermatogonial germline stem cells protect against kidney injury / Letizia De Chiara, Sharmila Fagoonee, Andrea Ranghino, Stefania Bruno, Giovanni Camussi, Emanuela Tolosano, Lorenzo Silengo, Fiorella Altruda. - In: JOURNAL OF THE AMERICAN SOCIETY OF NEPHROLOGY. - ISSN 1533-3450. - ELETTRONICO. - (2014), pp. 0-0. [10.1681/ASN.2013040367]

Availability:

This version is available at: 2158/1357495 since: 2024-06-10T07:48:46Z

Published version:

DOI: 10.1681/ASN.2013040367

Terms of use:

Open Access

La pubblicazione è resa disponibile sotto le norme e i termini della licenza di deposito, secondo quanto stabilito dalla Policy per l'accesso aperto dell'Università degli Studi di Firenze (https://www.sba.unifi.it/upload/policy-oa-2016-1.pdf)

Publisher copyright claim:

Conformità alle politiche dell'editore / Compliance to publisher's policies

Questa versione della pubblicazione è conforme a quanto richiesto dalle politiche dell'editore in materia di copyright.

This version of the publication conforms to the publisher's copyright policies.

(Article begins on next page)

01 August 2024

Downloaded from http://journals.lww.com/jasn by BhDMf5ePHKav1zEoum1tQfN4a+kJLhEZgbsIHo4XMi0hCywCX1AWnYQp/IlQrHD3i3D0OdRyi7TvSFl4Cf3VC1y0abggQZXdgGj2MwlZLeI= on 06/10/2024

Renal Cells from Spermatogonial Germline Stem Cells Protect against Kidney Injury

Letizia De Chiara,* Sharmila Fagoonee,* Andrea Ranghino,† Stefania Bruno,* Giovanni Camussi,*‡ Emanuela Tolosano,* Lorenzo Silengo,* and Fiorella Altruda*

*Department of Molecular Biotechnology and Health Sciences, Molecular Biotechnology Center, and ‡Department of Medical Sciences, University of Torino, Torino, Italy; and †Division of Nephrology Dialysis and Transplantation, Department of Medical Sciences, San Giovanni Battista Hospital and University of Torino, Torino, Italy

ABSTRACT

Spermatogonial stem cells reside in specific niches within seminiferous tubules and continuously generate differentiating daughter cells for production of spermatozoa. Although spermatogonial stem cells are unipotent, these cells are able to spontaneously convert to germline cell–derived pluripotent stem cells (GPSCs) *in vitro*. GPSCs have many properties of embryonic stem cells and are highly plastic, but their therapeutic potential in tissue regeneration has not been fully explored. Using a novel renal epithelial differentiation protocol, we obtained GPSC-derived tubular-like cells (GTCs) that were functional *in vitro*, as demonstrated through transepithelial electrical resistance analysis. In mice, GTCs injected after ischemic renal injury homed to the renal parenchyma, and GTC-treated mice showed reduced renal oxidative stress, tubular apoptosis, and cortical damage and upregulated tubular expression of the antioxidant enzyme hemeoxygenase-1. Six weeks after ischemic injury, kidneys of GTC-treated mice had less fibrosis and inflammatory infiltrate than kidneys of vehicle-treated mice. In conclusion, we show that GPSCs can be differentiated into functionally active renal tubular-like cells that therapeutically prevent chronic ischemic damage *in vivo*, introducing the potential utility of GPSCs in regenerative cell therapy.

J Am Soc Nephrol 25: 316–328, 2014. doi: 10.1681/ASN.2013040367

AKI is a common complication characterized by a rapid reduction in kidney function that results in failure to maintain fluid. AKI is a potentially reversible disease. However, some patients recover incompletely from AKI, and these patients either continue undergoing dialysis or progress to CKD. Moreover, development of CKD can lead to ESRD. One of the main causes of AKI is ischemia/reperfusion injury (IRI).[1] IRI is a pathologic condition characterized by an initial restriction of blood supply followed by the subsequent restoration of perfusion and concomitant reoxygenation that is frequently associated with an exacerbation of tissue injury and a strong inflammatory response.[2] The cells within the renal parenchyma that suffer the most damage upon kidney ischemia are the proximal tubular cells. This is likely due to the presence of a brush border on these cells that increases cell surface area and sensitizes them to damage.

The recent discovery of the ability to reprogram adult cells into pluripotent stem cells (iPSCs) has profound therapeutic implications for diseases involving tissue damage and degeneration. Derivation of pluripotent stem cells from an adult source avoids several ethical concerns of obtaining such cells from embryos. However, efficient generation of iPSCs typically requires transduction of cells with reprogramming factors, including potent proto-oncogenes that can limit their therapeutic uses.[3] The existence of inherent epigenetic differences between iPSCs and regular embryonic stem cells (ESCs) can adversely affect iPSCs functionality.[4,5]

Received April 10, 2013. Accepted August 19, 2013.

Published online ahead of print. Publication date available at www.jasn.org.

Correspondence: Dr. Fiorella Altruda, Via Nizza 52, 10126 Torino, Italy. Email: fiorella.altruda@unito.it

Copyright © 2014 by the American Society of Nephrology

Downloaded from http://journals.lww.com/jasn by BhDMf5ePHKav1zEoum1tQfN4a+kJLhEZgbsIHo4XMi0hCywCX1AWnYQp/IlQrHD3i3D0OdRyi7TvSFl4Cf3VC1y0abggQZXdgGj2MwlZLeI= on 06/10/2024

We explored alternative sources for therapeutically relevant adult pluripotent stem cells, in particular, from germ cells of the testis. Spermatogonial stem cells (SSCs) from the mouse can be cultured for the long term *in vitro* while maintaining stem cell potential.[6,7] Under specific culture conditions, the unipotent SSCs spontaneously convert at low frequency into pluripotent embryonic-like stem cells, known as germline cell–derived pluripotent stem cells (GPSCs).[8–11] This conversion occurs spontaneously without transduction of reprogramming factors, and thus GPSCs can be a valuable adult source of pluripotent stem cells for therapy.

GPSCs share many features with ESCs[9] and show great plasticity, being able to differentiate *in vitro* into functional cardiomyocytes,[12] neurons,[13] hematopoietic cells,[14] hepatocytes,[15] and vascular cells,[16] although the therapeutic potential of GPSCs in tissue regeneration has not been extensively studied. It was also demonstrated that the unipotent SSCs were able to transdifferentiate into renal cells once injected directly in the parenchyma of kidney.[17] In addition, studies performed on ESCs and iPSCs[18–23] have provided evidence of expression of markers associated with early stages of embryonic kidney development.

Here we demonstrate that GPSCs can differentiate into functional renal tubular-like cells *in vitro*. We also tested the functional capabilities of these tubular-like cells derived from GPSCs (GTCs) in treatment of an *in vivo* model of kidney ischemia and demonstrate that they protect against both acute and chronic kidney damage.

RESULTS

GPSCs Differentiate into Renal Tubular Cells *In Vitro*

GPSCs were obtained as previously described.[15] To induce differentiation of GPSCs into renal tubular cells, embryoid bodies (EBs) were formed by static culture and a new, specific protocol was designed to induce renal tubular differentiation (Figure 1). EBs were assessed at various differentiation days for the expression of genes involved in kidney development.[20] The genes were analyzed by real-time PCR and immunofluorescence, as listed: brachyury and goosecoid as markers of mesodermal layer; vimentin as marker of mesenchymal-derived cells; cadherin-16/kidney-specific protein (KSP), Tamm-Horsfall protein (THP), and mineralocorticoid receptor as markers of tubular epithelial cells, and podocalyxin, nephrin, Wt1, and aquaporin-2 as markers of podocytes, glomerular cells, and collecting duct cells, respectively. After 6 days in suspension, EBs start to develop the mesodermal layer, as confirmed by the expression of brachyury (Figure 2A) and goosecoid. The expression of goosecoid dropped at day 14 (Figure 2C), whereas brachyury was expressed until day 35 (Figure 2B). Vimentin (Figure 2D) was highly expressed from day 14 and remained stable. Because vimentin is usually not expressed in differentiated tubular cells, the stable expression of this marker (Figure 2, D and H) in our culture highlights that these cells are not fully differentiated and that they are closer to progenitor cells. At day 21, we detected the expression of cadherin-16/KSP by real-time PCR (Figure 2F) and immunofluorescence analysis[24] (Figure 2I). Cadherin-16 is expressed specifically in renal tubular cells, and *in vivo* its expression starts at the S-shaped body stage, around E14.5 in mice.[25] THP, the most abundant protein secreted in the urine, was detected by immunofluorescence (Figure 2J) starting from day 28. Mineralocorticoid receptor was expressed consistently from day 21 (Figure 2E). During differentiation, GPSCs underwent a process of tubulogenesis stimulated by collagen type IV, a component of the renal basal membrane, that was used to coat the culture plates. Epidermal growth factor (EGF) is another key factor involved in this process. The EGF added to the culture medium not only was able to stimulate cell proliferation but was also crucial for formation of tubular-like structures.[26] Tubular-like structures started to appear at day 21 (Figure 2G). Similar structures were formed by baby mouse kidney epithelial cells in tridimensional culture.[26]

Furthermore, we investigated by real-time PCR analysis the expression of podocalyxin, nephrin, Wt1, and aquaporin-2. These markers were expressed only within the first two weeks of culture and dropped after the treatment of EBs with the conditioned medium (Supplemental Figure 1), with the exception of aquaporin-2, which was undetectable (data not shown). Thus, we demonstrated that GTCs express only markers specific for renal tubular cells.

To obtain a pure population of tubular-like cells, we isolated KSP^+ cells from EBs at day 35 of differentiation. The cells were sorted, taking advantage of the magnetic-activated cell sorting (MACS) method. The KSP^+ cells strongly expressed KSP (Figure 2L), mineralocorticoid receptor (Supplemental Figure 2A) but not oct4, Wt1, goosecoid, and podocalyxin (Supplemental Figure 2, B–E). KSP^+ cells expressed vimentin at a very

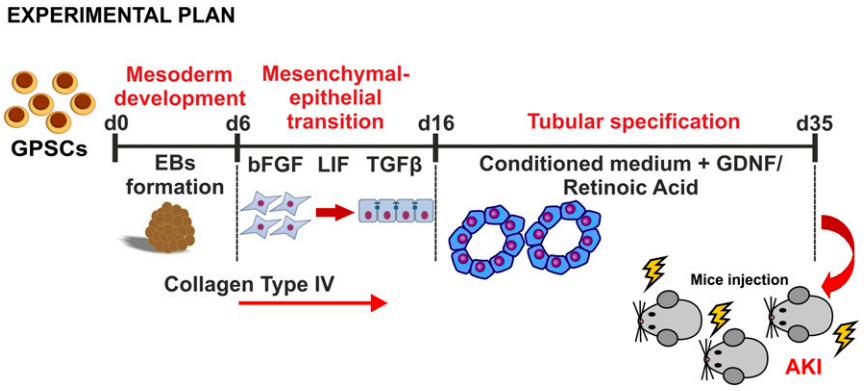

Figure 1. Experimental plan shows that GPSCs are differentiated toward renal tubular cells and injected in IRI mice after 35 days. FGF, fibroblast growth factor; GDNF, glial cell–derived neurotrophic factor.

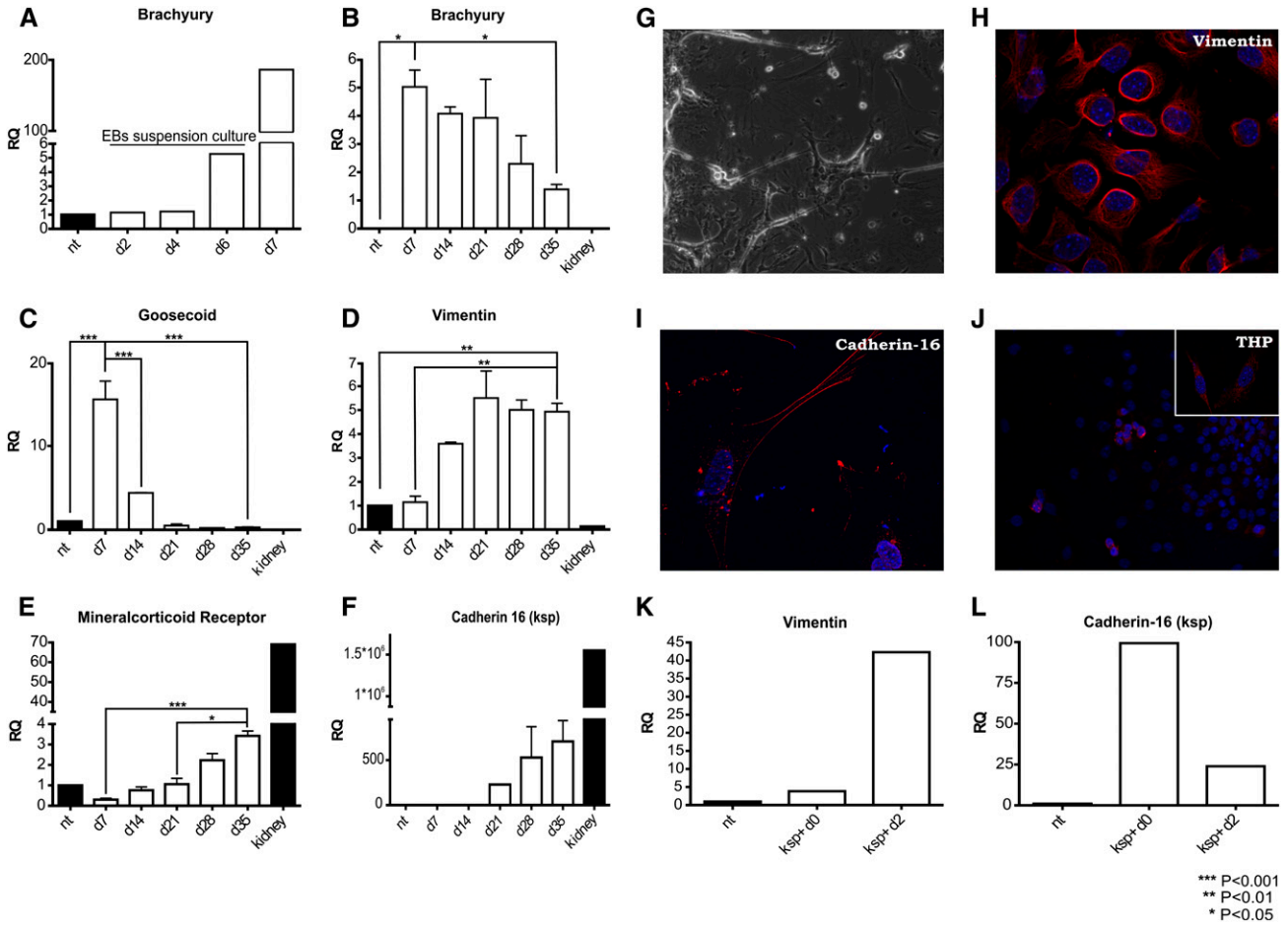

Figure 2. GTCs show a renal tubular epithelial phenotype. RNA was extracted at different time points, and real-time PCR analysis (A–F) was performed. The mesodermal marker Brachyury began to be expressed after 6 days in suspension (A) and decreased during the culture (B). Goosecoid, another mesodermal marker, is undetectable starting from day 21 (C). Vimentin, a marker of mesenchymal-derived cells, is stably expressed for the whole duration of the culture (D). Mineralocorticoid receptor (E) and cadherin-16/KSP (F) are expressed consistently from day 21 until day 35 of the EB culture. Each column refers to three independent samples. Tubular-like structures (G) appear spontaneously after 21 days in culture (original magnification ×100). We assessed the expression of vimentin (H), KSP (I), and THP (J) through immunofluorescence staining. Nuclei were counterstained in DAPI. (Original magnification: THP ×400, vimentin/KSP ×630.) Finally, we evaluated the expression pattern of KSP^+ cells. After 2 days in the absence of EB environment, cells start to dedifferentiate, as demonstrated by the decrease of cadherin-16/KSP (L) and the increase of vimentin (K) expression. (KSP^+ d0: RNA was extracted immediately after isolation; KSP^+ d2: RNA was extracted 2 days after cells isolation.) Data are presented as mean ± SEM.

low level (Figure 2K), indicating that this fraction of cells represents the most differentiated cells in EBs. Two days after MACS isolation, the KSP^+ cells started to dedifferentiate, as demonstrated by the re-expression of vimentin. This highlights the importance of the EB environment in supporting the differentiation process of tubular-like cells.

Transepithelial Electrical Resistance Measurement Confirms That GTCs Are Functional Epithelial Cells

To assess functionality of the GTCs, we measured transepithelial electrical resistance (TEER), which indicates the presence of tight junctions that are typical structures of epithelial cells.[27–29] Similar results were obtained from three independent experiments. Different fractions of cells were analyzed: (*1*) the "unsorted" fraction, representing the trypsinized and replated EBs, and thus composed of both the KSP^+ and KSP^- cells; (*2*) KSP^+ fraction, composed of cells recovered from MACS; (*3*) KSP^- fraction, composed of unbound cells collected from MACS; (*4*) undifferentiated GPSCs as negative control; and (*5*) mouse primary renal tubular cells as positive control.

In KSP^+ cells fraction and mouse primary tubular cells TEER measurement was similar (Figure 3). The high level of TEER measurement found in the KSP^+ fraction was a result of their ability to form tight junctions as confirmed by the immunofluorescence analysis for Zonula Occludens protein-1 (ZO-1) (Supplemental Figure 3), a marker of tight junction.

Teratoma Formation Assay

At day 42 of differentiation, GTCs were assessed for their ability to induce teratomas. To test teratoma development, mice were

Downloaded from http://journals.lww.com/jasn by BhDMf5ePHKav1zEoum1tQfN4a+kJLhEZgbsIHo4XMi0hCywCX1AWnYQp/IlQrHD3i3D0OdRyi7TvSFl4Cf3VC1y0abggQZXdgGj2MwlZLeI= on 06/10/2024

Downloaded from http://journals.lww.com/jasn by BhDMf5ePHKav1zEoum1tQfN4a+kJLhEZgbsIHo4XMi0hCywCX1AWnYQp/IlQrHD3i3D0OdRyi7TvSFl4Cf3VC1y0abggQZXdgGj2MwlZLeI= on 06/10/2024

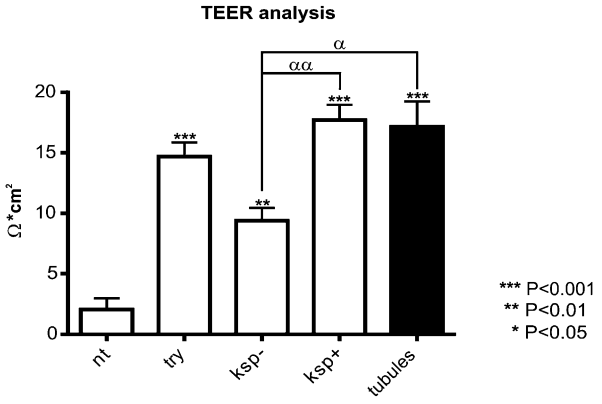

Figure 3. GTCs are functional epithelial cells. The panel (A) shows the measure of TEER among different fractions of cells. It is representative of three independent experiments (n=4 each column). The asterisks represents the statistical difference between every fraction and undifferentiated GSPC (NT) fraction. α represents statistically relevant difference among cells fractions with the exception of NT fraction. Data are presented as mean ± SEM. KSP^+, cells recovered from MACS; KSP^-, unbound, negative fraction recovered from MACS; try, whole EBs trypsinized and replated.

injected under left renal capsule with 1×10^6 GTCs or undifferentiated GPSCs, as positive control. After 6 weeks, all kidneys injected with undifferentiated GPSCs showed prominent teratomas (Figure 4A), visible by eye inspection.[9,10,30] The analysis of hematoxylin and eosin–stained sections showed the presence of structures derived from mesodermal, ectodermal, and endodermal layers (data not shown). On the contrary, kidneys injected with GTCs did not show teratoma formation (Figure 4B).

GTCs Protect against AKI

To investigate whether GTCs could protect against AKI, we chose a model of IRI based on unilateral nephrectomy followed by left kidney ischemia. After damage, we injected GTCs in female mice through the tail vein. GTCs labeled with Vybrant CFDA SE Cell Tracer Kit (CFSE) (Molecular Probes, Leiden, The Netherlands) were detected in renal parenchyma 48 hours after injection, showing their capacity to home injured kidney (Figure 5). The homing ability of GTCs was confirmed by *in situ* analysis of Y chromosome. GTCs positive for Y chromosome were detected in renal parenchyma 2 days after injection (Figure 6B) and represented 1.5% of the total number of nuclei. Six weeks after IRI, the number of Y^+ cells, mostly located in the tubular structures (Figure 6C), was 2% of total number of nuclei. This percentage was slightly higher than that of Y^+ cells after 48 hours (Supplemental Figure 4E). Double staining for Y chromosome and BrdU 48 hours after IRI revealed that although Y^+ cells were able to proliferate, the number of $BrdU^+/Y^+$ was lower than the total number of proliferating cells (Supplemental Figure 4, C and D).

Ischemized mice injected with GTCs showed significant reduction in BUN ($P<0.01$) and creatinine ($P<0.05$) levels compared with control mice injected with PBS (Figure 7A).

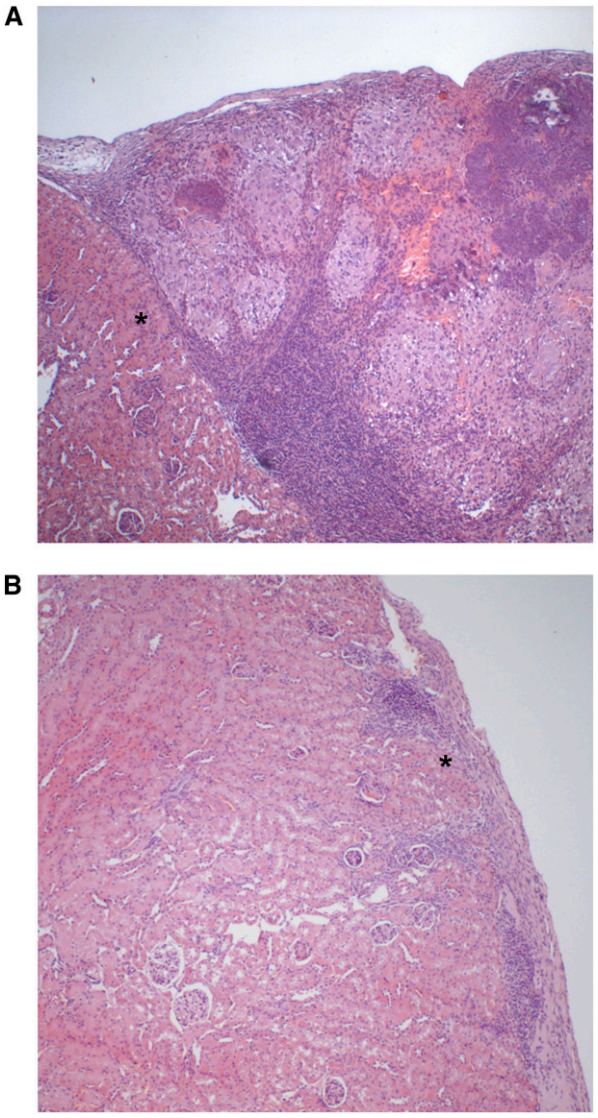

Figure 4. GTCs do not form teratomas *in vivo*. Representative hematoxylin and eosin staining of teratoma formation assay in the left kidney of mice injected with GPSCs (A) and GTCs after 42 days of differentiation (B). The images show the lack of teratoma formation in mice injected with GTCs, whereas mice injected with undifferentiated GPSCs show a prominent teratoma. *Same region of the two kidneys. (Original magnification ×40.)

Histologic analysis of IRI kidneys revealed a marked reduction of tissue damage in GTC-injected mice with respect to that of PBS-injected mice (Figure 7B). The number of CASTs (hyaline material inside the tubular lumen that block and impair the tubular functionality) and necrotic tubules in the renal cortex of mice treated with GTCs was significantly lower ($P<0.001$) compared with PBS-injected mice (Figure 7C). Moreover, apoptotic cells were reduced in IRI mice treated with GTCs ($P<0.05$), suggesting an antiapoptotic effect of GTCs on tubular cells (Figure 7G). In association with this result, we found that the number of tubules expressing hemeoxygenase-1 (HO-1), a well known protective enzyme that exerts an activity against

Downloaded from http://journals.lww.com/jasn by BhDMf5ePHKav1zEoum1tQfN4a+kJLhEZgbsIHo4XMi0hCywCX1AWnYQp/IlQrHD3i3D0OdRyi7TvSFl4Cf3VC1y0abggQZXdgGj2MwlZLeI= on 06/10/2024

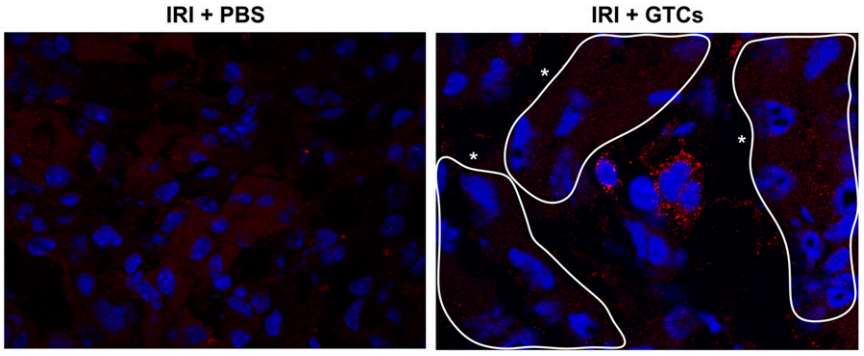

Figure 5. GTCs are able to reach the injured kidney and migrate in the renal parenchyma. GTCs labeled with CFSE are present in renal parenchyma 48 hours after ischemia. $CFSE^+$ cells are found to be localized among the tubules. No signal is detected in PBS-injected mice. *Tubules. $CFSE^+$ cells are revealed with a secondary antibody Alexa 565; nuclei are counterstained with DAPI. (Original magnification ×630.)

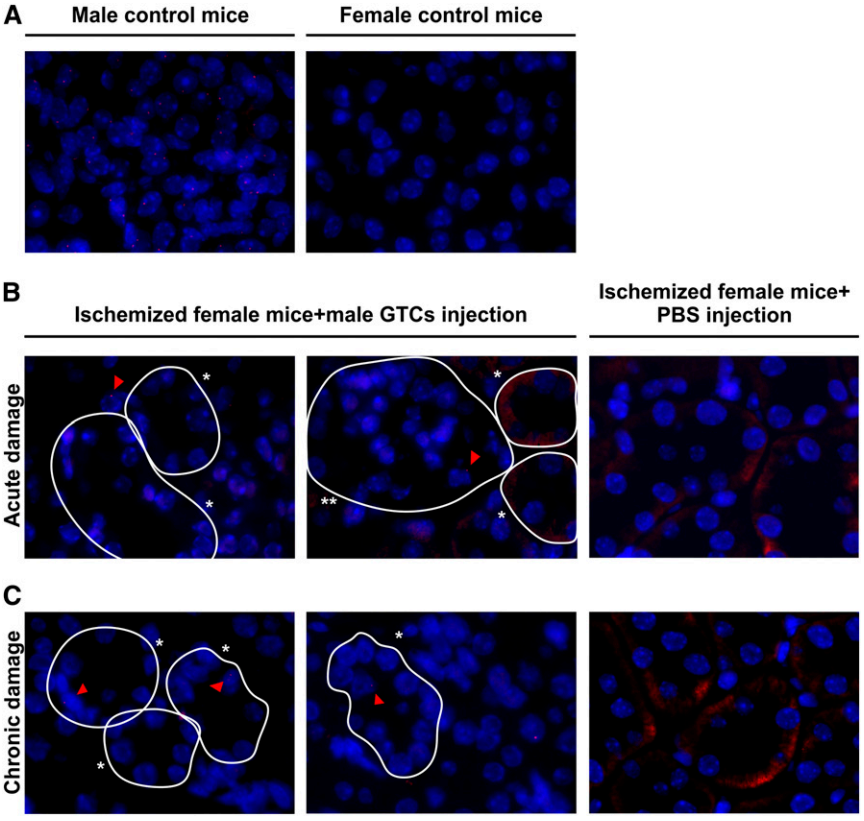

Figure 6. GTCs Y^+ cells are detected in different site of renal parenchyma in acute and chronic experiments. The upper panel (A) shows a positive control on the left and a negative control on the right, demonstrating that the probe for Y chromosome is specific. After 48 hours (acute damage), the cells are mostly in the glomeruli and in the interstitial space between tubules (B). *Tubules; **glomeruli. Six weeks after ischemia (chronic damage), GTCs Y^+ cells are detected in the tubular structures (C), indicating that GTCs are able to home and engraft the damaged renal tubules. Ischemized female mice injected with PBS do not show any positive signal. (Original magnification, ×1000; nuclei are counterstained with DAPI.) Red triangles indicate the red spot of the Y chromosome.

oxidative stress,[31] was increased in GTC-treated mice (Figure 7F) compared with mice injected with PBS ($P<0.01$), and this result was also confirmed by real-time PCR analysis ($P<0.05$) (Supplemental Figure 5A). Cell proliferation and $CD18^+$ infiltration did not show any difference in GTCs or PBS injected mice (Supplemental Figure 5, B and C).

To evaluate the contribution of GTCs to the repair process, undifferentiated GPSCs or KSP^+ cells 4 days after MACS isolation were injected after IRI. Injection of GPSCs did not affect renal functionality or HO-1 expression (Supplemental Figure 6), whereas KSP^+ cells up-regulated HO-1 (Supplemental Figure 7) albeit less markedly versus differentiated GTCs.

Taken together, these results demonstrate that GTCs can protect against AKI caused by ischemic damage.

GTCs Protect against CKD

It is known that AKI can trigger CKD.[32,33] To test the possibility that the treatment with GTCs could protect against chronic disease progression, we evaluated kidney functionality and histology in mice injected with GTCs 6 weeks after IRI-AKI. We scored the percentage of mice in the groups of GTC/PBS-injected mice that developed chronic renal damage. The scoring of CKD highlighted that GTC-injected mice were less prone to develop a chronic disease (Figure 8A).

To confirm the damaging of left kidney after ischemic insult, we analyzed BUN and creatinine levels after 48 hours (data not shown). Six weeks after IRI, BUN and creatinine levels were decreased in both groups compared with levels measured 48 hours after IRI. We did not find any significant difference between mice treated with GTCs and those injected with PBS alone (Figure 8, C and D). In fact, it is known that BUN and creatinine levels are normal until 60% of total kidney function is lost. On the other hand, measurement of cystatin C, a more accurate marker of renal functionality, revealed that serum cystatin C was significantly lower ($P<0.01$) in mice treated with GTCs than those injected with PBS alone (Figure 8E). As expected, the relative kidney weight did not differ significantly between ischemized mice treated

Downloaded from http://journals.lww.com/jasn by BhDMf5ePHKav1zEoum1tQfN4a+kJLhEZgbsIHo4XMi0hCywCX1AWnYQp/IlQrHD3i3D0OdRyi7TvSFl4Cf3VC1y0abggQZXdgGj2MwlZLeI= on 06/10/2024

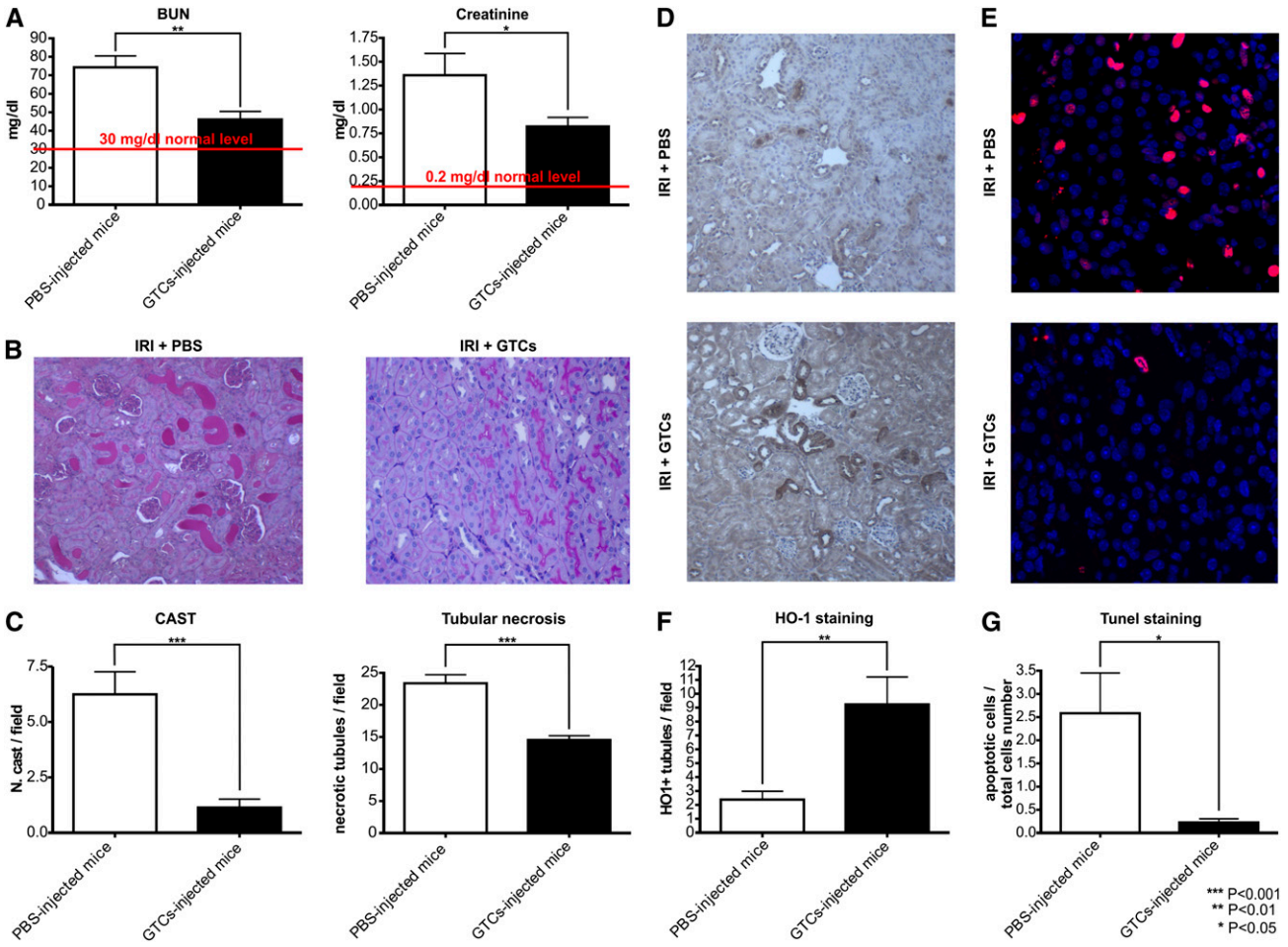

Figure 7. GTCs protect kidney from AKI through HO-1 upregulation. BUN and creatinine (A) levels in the blood of mice injected with GTCs are significantly lower than those in mice injected with PBS. GTC-injected mice show a reduction of cortical damage (B), as shown by periodic acid–Schiff staining (original magnification, ×200) compared with PBS-injected mice. GTC-treated mice also show a lower incidence of tubular necrosis (C) than PBS-injected mice; the left chart indicates incidence of CAST formation, and the right chart represents the total number of necrotic tubules (tubules undergoing necrosis plus CAST). HO-1 is upregulated in GTC-treated mice compared with PBS-injected mice (D), and apoptotic ratio is decreased (E) (original magnification: HO-1, ×100; TUNEL staining, ×630). The lower panel represents the quantification of HO-1$^+$ (F) tubules and apoptotic cells (G). Data are presented as mean ± SEM. (GTC-injected mice, *n*=8; PBS-injected mice, *n*=8.)

with GTCs or with PBS.[34] Whereas the relative kidney weight was significantly decreased in ischemized mice injected only with PBS compared with the control nonischemized mice ($P<0.05$) (Figure 8B). Tubular dilation/cyst analysis indicated that tubular dilation type I ($P<0.01$) and microcysts ($P<0.01$) formation were significantly lower in mice injected with GTCs than in PBS-injected mice (Figure 9, B and C). In addition, cyst formation could be detected only in mice injected with PBS but not in mice treated with GTCs ($P<0.01$) (Figure 9C). Because persistent infiltration is a factor linked to fibrogenesis and chronic disease development, we evaluated the inflammatory infiltrates in ischemized and control kidneys. The percentage of infiltrating cells (CD18$^+$ cells) was significantly ($P<0.01$) lower in mice injected with GTCs than in mice injected with PBS (Figure 10, C and D). Moreover, picrosirius red staining[35–37] revealed that mice injected with GTCs developed less fibrosis than mice injected with PBS (Figure 10, A and B). This result was confirmed by the quantification of fibrotic area in renal sections of mice injected or not injected with GTCs ($P<0.05$) stained with Masson trichrome (Figure 10G). Finally, the incidence of glomerular sclerosis and tubular atrophy was lower ($P<0.05$) in mice injected with GTCs compared with mice injected with PBS (Figure 10, E and F). Together, these results demonstrate that treatment with GTCs protect the kidney against IRI-induced chronic disease.

DISCUSSION

Adult stem cells have great plasticity, providing an opportunity for the treatment of a wide range of diseases,[38–40] representing an alternative to ESCs in regenerative cell therapy. In particular,

Downloaded from http://journals.lww.com/jasn by BhDMf5ePHKav1zEoum1tQfN4a+kJLhEZgbsIHo4XMi0hCywCX1AWnYQp/IlQrHD3i3D0OdRyi7TvSFl4Cf3VC1y0abggQZXdgGj2MwlZLeI= on 06/10/2024

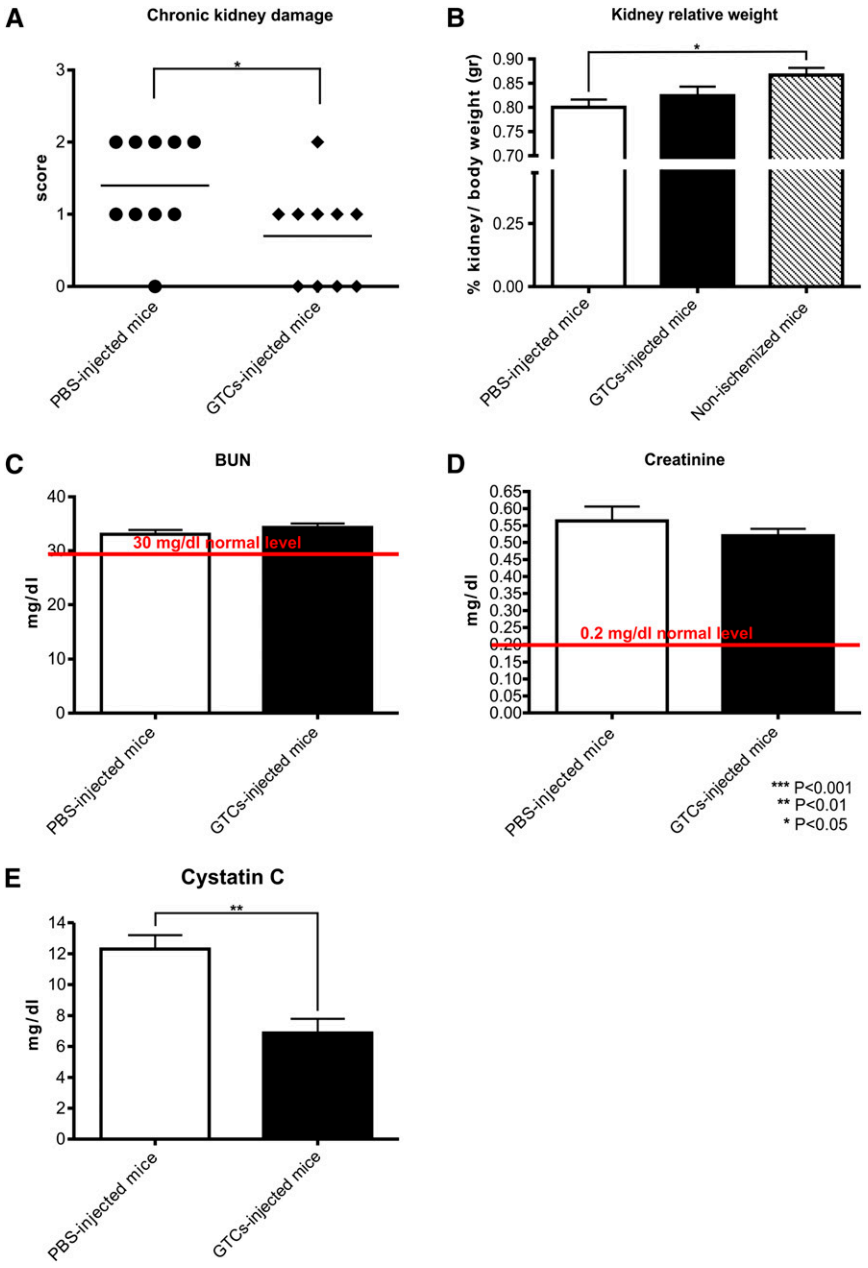

Figure 8. Mice injected with GTCs are protected against CKD development. The score (A) shows that ischemized mice injected with PBS are more prone to develop a chronic disease. The relative kidney weight (B) does not differ between mice treated with GTCs and those treated with PBS, but it is decreased in mice injected only with PBS compared with the control nonischemizedmice. The relative percentage of kidney weight is evaluated on the total body weight of the mice. BUN (C) and creatinine (D) analysis shows no difference between mice injected or not injected with GTCs 6 weeks after ischemia. BUN returns to normal level whereas creatinine remains slightly higher. Cystatin C (E) is downregulated in mice injected with GTCs compared with mice injected with PBS (PBS-injected mice, *n*=10; GTC-injected mice, *n*=10; nonischemized mice, *n*=4). Data are presented as mean ± SEM.

GPSCs have aroused a growing interest in the recent years.[41–44] Murine GPSCs resemble ESCs in colony morphology, in their ability to form all the three germ layers and teratomas *in vivo*.[8–10]

In this study, we demonstrate the differentiation of murine GPSCs, *in vitro,* into renal tubular-like cells and their ability, *in vivo*, to restore kidney function after AKI. After 6 days in culture, EBs start to express mesodermal genes. Then, as a result of the treatment with the conditioned medium, a small fraction of EBs shifts toward a more differentiated state, expressing genes such as *KSP* and mineralocorticoid receptor. KSP is a cadherin expressed exclusively in renal tubular epithelial cells.[45] The number of cells expressing KSP protein is about 10% of the total cell population (data not shown). More specific differentiating factors in the medium are needed to increase the number of KSP^+ cells.

GTCs stably express vimentin-like immature progenitor tubular cells. Vimentin, normally not present in the adult renal tubular cells, starts to be expressed at a high level within the first days after severe injury, during the repair process. In this process, renal tubular cells recapitulate gene expression patterns typical of the developing nephron.[1,46] This observation may have important implications in the use of GTCs in kidney repair.

To test the functionality of the GTCs *in vivo*, we chose the renal IRI as a model of renal failure. After damage induction, we injected GTCs at day 35 of differentiation into the tail vein of female mice. *In situ* analysis of Y chromosome on the renal parenchyma of female mice demonstrates that transplanted male GTCs are able to reach the injured kidney and migrate in the renal parenchyma. Y^+ cells are present in renal parenchyma 48 hours after ischemia, mostly in the interstitial area or inside the glomeruli. After 6 weeks, cells positive for the Y chromosome persisted in tubules, indicating a long-term engraftment of these cells in renal parenchyma. We found that the percentage of engrafted cells is increased 6 weeks after IRI compared with 48 hours after IRI. Although 48-hour IRI mice display a small amount of double-positive staining for both Y chromosome and BrdU, we could not detect any adjacent Y^+ cells or $Y^+/BrdU^+$ cells 6 weeks after IRI. These results indicate that GTC proliferation is not a prominent event involved in kidney repair.

Renal ischemic injury permanently damages peritubular capillaries, causing hypoxia, which may be involved in the progression of CKD after AKI.[47] HO-1 is an inducible enzyme

Downloaded from http://journals.lww.com/jasn by BhDMf5ePHKav1zEoum1tQfN4a+kJLhEZgbsIHo4XMi0hCywCX1AWnYQp/IlQrHD3i3D0OdRyi7TvSFl4Cf3VC1y0abggQZXdgGj2MwlZLeI= on 06/10/2024

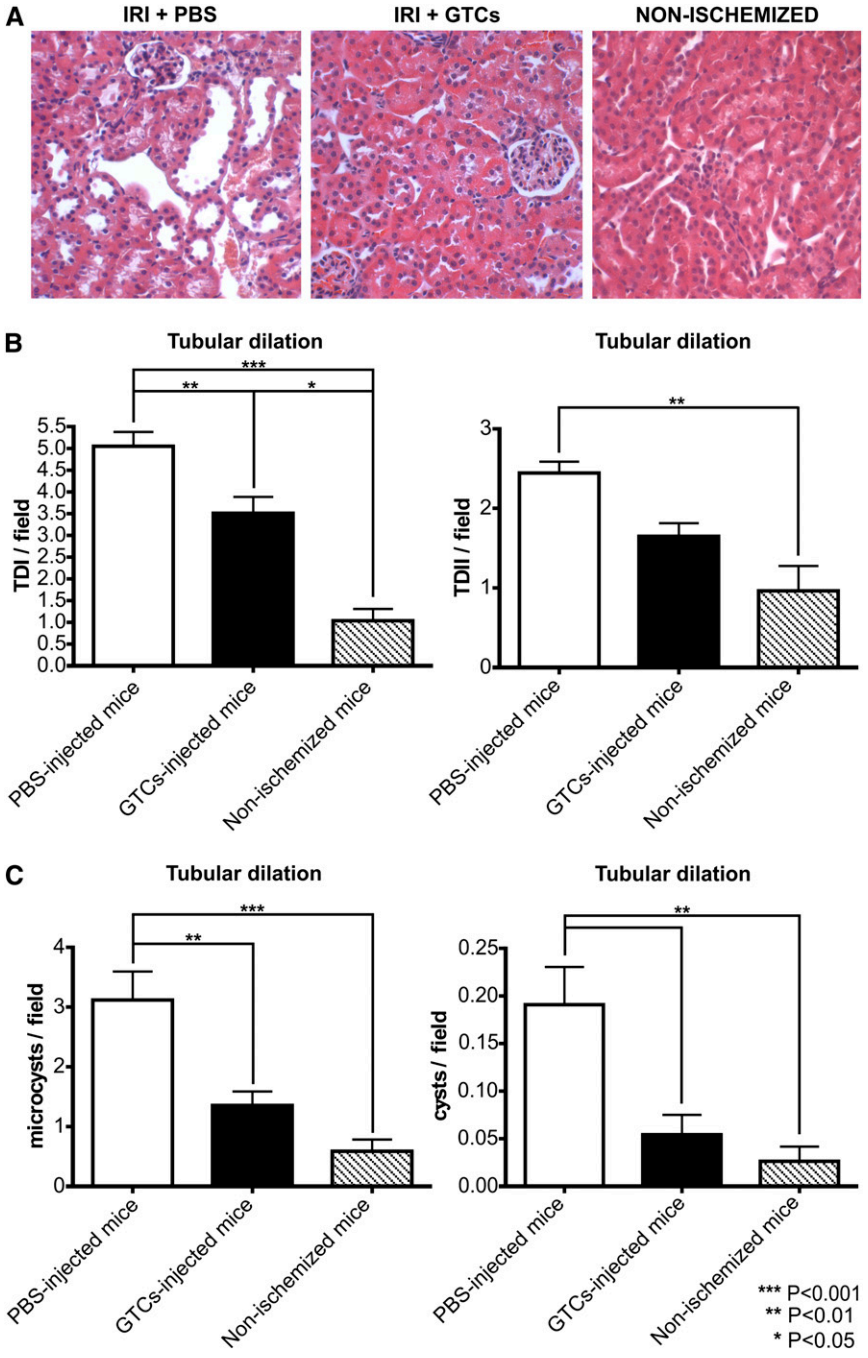

Figure 9. Mice injected with GTCs do not showtubular dilation. Representative hematoxylin and eosin staining (A) of kidney cortical sections of ischemized mice 6 weeks after ischemia and of a healthymouse (original magnification, ×200). The charts below show the quantification of tubular dilation (B and C). In particular, the amount of microcysts and cysts in mice injected with GTCs is similar to that in nonischemized healthy mice (PBS-injected mice, *n*=10; GTC-injected mice, *n*=10; nonischemized mice, *n*=4). Data are presented as mean ± SEM.

that protects against oxidative stress, regulating cellular respiration and oxygen availability,[48] and its upregulation is linked to a decrease in the apoptotic ratio.[31,49] The expression of HO-1 is always correlated with a better prognosis after ischemic damage.[50–52] We found that mice injected with GTCs showed a strong upregulation of HO-1 2 days after renal damage induction. This finding suggests that HO-1 upregulation induced by GTCs could be involved in kidney protection from IRI. A high level of expression of HO-1 after ischemic insult is related to less impairment of renal parenchyma and fewer apoptotic cells because of the antiapoptotic role of HO-1. Our results support the hypothesis that the upregulation of HO-1 in mouse kidneys treated with GTCs may be the mechanism involved in functional kidney protection. Interestingly, the intravenous injection of KSP^+ cells helped protect against AKI, resulting in an intermediate phenotype compared with that of GPSCs and differentiated GTCs. This result confirmed that the effect is specific because the injection of undifferentiated GPSCs cannot protect kidneys against IRI.

After a single kidney ischemic event, patients can develop CKD.[32,33] Chronic damage is accompanied by loss of kidney weight, tubular dilation, and persistent inflammation that lead to the release of profibrogenic factors.[32,35] Usually the kidney is able to restore normal functionality,[35] and the main challenge is to prevent fibrosis progression. Six weeks after ischemia, fibrosis, together with tubular dilation, glomerular sclerosis, and tubular atrophy, was almost absent in the renal parenchyma of mice injected with GTCs. These factors are important hallmarks of chronic disease, and their absence confirm the role of GTCs in protecting kidney from CKD progression.

We did not detect any differences in kidney weight between ischemized mice injected or not injected with GTCs. The explanation could reside in the strong compensative hypertrophic stimulus consequence of the presence of a single kidney,[34] as dictated by our IRI model.

In conclusion, these data show that GTCs can be derived from GPSCs and that they are functionally active *in vivo* for the repair of renal damage in a murine model of IRI. These findings open the possibility to repair damage in acute renal disease, with the advantage of using GPSCs directly isolated from patients. Furthermore, because of the high plasticity displayed by GPSCs, the hope is that these cells could be applied to other diseases.

Downloaded from http://journals.lww.com/jasn by BhDMf5ePHKav1zEoum1tQfN4a+kJLhEZgbsIHo4XMi0hCywCX1AWnYQp/IlQrHD3i3D0OdRyi7TvSFl4Cf3VC1y0abggQZXdgGj2MwlZLeI= on 06/10/2024

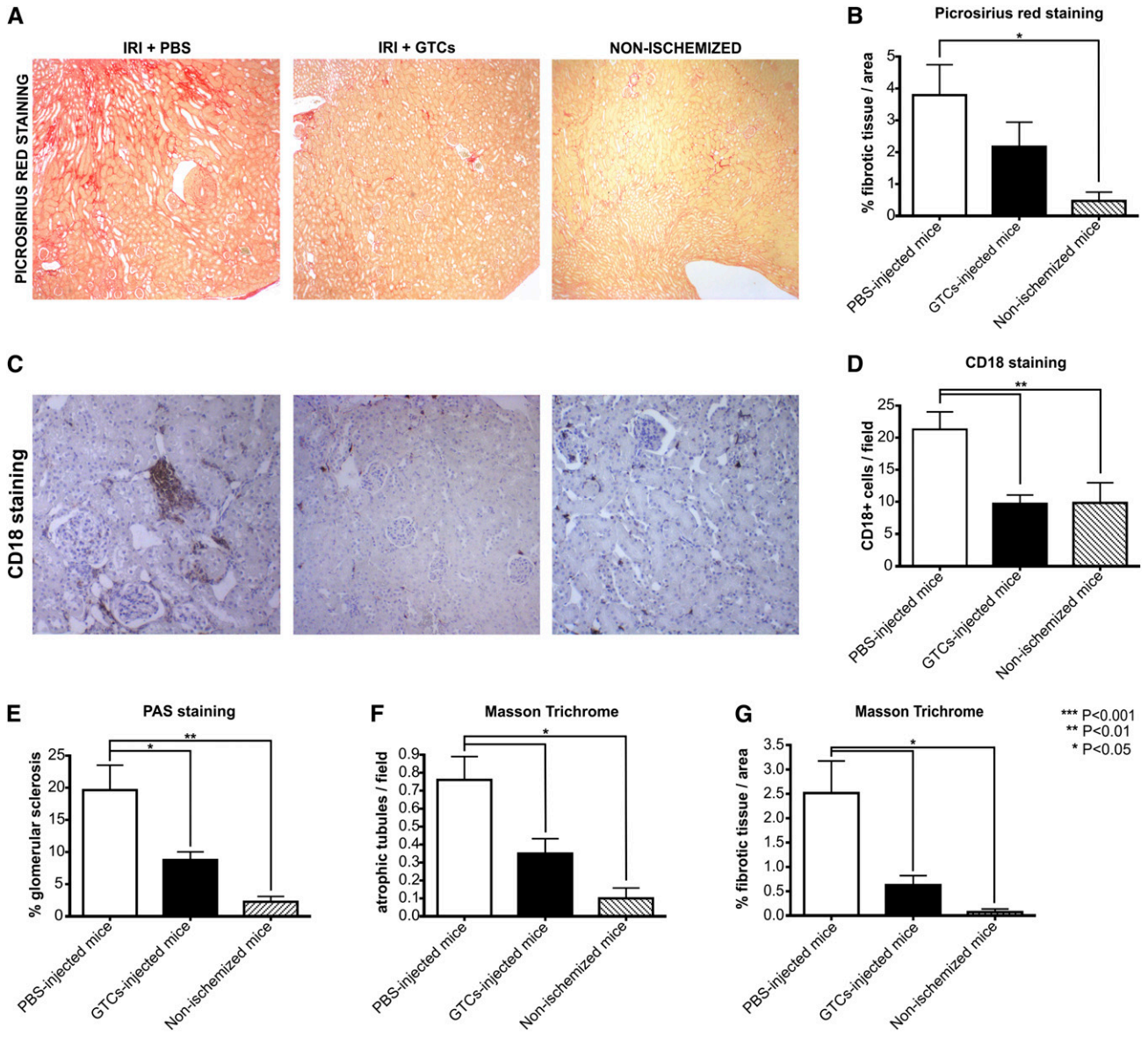

Figure 10. GTCs injection in mice prevent renal fibrogenesis. The upper panel (A) shows three representative pictures of fibrotic tissue in ischemized mice and healthy nonischemized mice, stained with picrosirius red. The lower panel (C) shows, for the same mice, the presence of infiltrating $CD18^+$ cells and quantification of infiltrating cells per field (D). (Original magnification: picrosirius red, ×40; $CD18^+$, ×100.) The quantification of fibrogenesis (B) is performed through MetaMorph software, and results are expressed as the mean ratio of the stained area to the total tissue area. Evaluation of renal fibrotic area on Masson trichrome staining (G) confirms the result obtained with picrosirius red staining. Glomerular sclerosis (E) and tubular atrophy are also evaluated (F). The number of sclerotic glomeruli and atrophic tubules is significantly decreased in the ischemized mice injected with GTCs compared with PBS-injected mice. (PBS-injected mice, n=10; GTC-injected mice, n=10; nonischemized mice, n=4.) Data are presented as mean ± SEM. $CD18^+$ is the marker for all the infiltrating cells.

CONCISE METHODS

Culture of Undifferentiated GPSCs and EB Formation

GPSCs were maintained in DMEM (Invitrogen), 15% FBS (HyClone FBS characterized; Thermo Scientific), with 1000 U leukemia inhibitory factor per liter.[9] EB formation was induced by seeding 500 cells/50 μl in an ultra-low-attachment 96-well plate (Corning, Lowell, MA). EBs were maintained in 1:1 DMEM/F12:RPMI (Invitrogen) containing 0.01 mM nonessential amino acid (Gibco), 1 mM sodium pyruvate (Gibco), 100 U/ml penicillin (Gibco), 100 μg/ml streptomycin (Gibco), 0.1% BSA fraction V (Gibco), 0.05 mM 2-β mercaptoethanol (Sigma-Aldrich) (basal medium composition), and 10% FBS for 6 days in suspension, allowing mesoderm induction; medium was added every 2 days.

Downloaded from http://journals.lww.com/jasn by BhDMf5ePHKav1zEoum1tQfN4a+kJLhEZgbsIHo4XMi0hCywCX1AWnYQp/IlQrHD3i3D0OdRyi7TvSFl4Cf3VC1y0abggQZXdgGj2MwlZLeI= on 06/10/2024

Renal Tubular Differentiation of GPSCs *In Vitro*

After mesoderm induction, EBs were plated on collagen 10 $\mu g/cm^2$ (collagen type IV from human placenta; Sigma-Aldrich).[53] EBs were cultured from day 6 to day 16 in 1:1 DMEM/F12:RPMI (Invitrogen) containing the basal medium components, a "nephrogenic cocktail"[54] of fibroblast growth factor-2 (50 ng/ml; Voden), TGF-β (4 ng/ml; PeProtech), leukemia inhibitory factor (20 ng/ml), and low serum concentration (1%). Starting from day 16, EBs were stimulated with a conditioned medium collected from primary renal tubular cells cultured as described below. Several factors were added to the medium: 1% FBS, EGF (10 ng/ml; PeProtech)[26]; a cocktail of insulin, transferrin, and sodium selenite 10 μg/ml, 5.5 μg/ml, and 5 ng/ml, respectively; ITS 100×; Sigma-Aldrich); hydrocortisone (36 $\mu g/\mu l$; Sigma-Aldrich); glial cell line–derived neurotrophic factor (50 ng/μl; PeProtech)[22]; retinoic acid (10^{-7} M; Sigma-Aldrich); glucose (0.15 g; Sigma-Aldrich)[55]; and all components of the basal medium (Figure 1).

Culture of Mouse Primary Renal Tubular Cells

Primary renal tubular cells were isolated under sterile conditions from kidneys of 129sv mice (8 weeks old) by a modification of previously described methods.[56] Renal cortex was sliced with surgical scalpel and then passed in three different filters to achieve tubular cells isolation (50 mesh, 70 μm, 40 μm). Primary tubular cells were maintained in DMEM to which 15% serum was added. When the cells reached 60%–70% of confluence, they were rinsed with PBS and then starved for 24 hours in DMEM containing only 0.1% BSA. The conditioned medium was collected 24 hours after starvation and centrifuged at 3000 rpm for 10 minutes to remove the debris. Two collections were performed for each plate.

Analysis of mRNA Expression

Total RNA was extracted from EBs at days 2, 4, 6, 7, 14, 21, 28, and 35 according to the manufacturer's instruction (PureLink RNA Mini Kit; Invitrogen). Primary renal tubules and kidneys were used as positive controls.

For the analysis of HO-1 mRNA, total RNA was extracted from kidneys 48 hours after ischemia, according to manufacturer's instruction (TRI Reagent; Ambion). cDNA was synthesized starting from 500 ng of RNA, as previously described.[15] Quantitative real-time-PCR was performed using primers listed in Table 1.

Immunofluorescence Staining

EBs were fixed with 4% paraformaldehyde for 10 minutes; all the primary antibodies were diluted in 1% BSA (Sigma-Aldrich) and incubated for 1 hour at room temperature. The following antibodies were used: goat polyclonal anti-KSP (cadherin-16; Santa Cruz Biotechnology), rabbit polyclonal anti-THP (Uromodulin; Santa Cruz Biotechnology), goat polyclonal antivimentin (Santa Cruz Biotechnology), rabbit polyclonal anti–ZO-1 (Invitrogen). Nuclei were counterstained with DAPI (Sigma-Aldrich).

Isolation of KSP^+ Cells

KSP^+ cells were isolated from EB culture using MACS (Miltenyi Biotec). The cell suspension was incubated with KSP (cadherin-16; Santa Cruz Biotechnology) primary antibody, 1 μl of antibody/10^6 cells, then washed in buffer. Two-cell suspensions were obtained: the labeled fraction (KSP^+ cells) and the unlabeled fraction (KSP^- cells).

Table 1. Primers used for PCR

Transcript	Sequence (5′-3′)	Bases
Brachyury	GAGCCTGGGGTGATGGTA	20
	CAGCCCACCTACTGGTCTTA	20
Cadherin-16/KSP	GGTTGTCCACCATGATACCC	20
	TGCAGCGACACACAATCAC	19
Goosecoid	GAGACGAAGTACCCAGACGTG	21
	GCGGTTCTTAAACCAGACCTC	21
HO-1	GGTCAGGTGTCCAGAGAAGG	20
	CTTCCAGGGCCGTGTAGATA	20
Mineralocorticoid receptor	CAAAAGAGCCGTGGAAGG	18
	TTTCTCCGAATCTTATCAATAATGC	25
Nephrin	AACATCCAGCTCGTCAGCAT	20
	AGGGCTCACGCTCACAAC	18
Podocalyxin	TCCTTGTTGCTGCCCTCT	18
	CTCTGTGAGCCGTTGCTG	18
Vimentin	CCAACCTTTTCTTCCCTGAA	20
	TGAGTGGGTGTCAACCAGAG	20
Wt1	CAGATGAACCTAGGAGGAGCTACCTTAAA	26
	TGCCCTTCTGTCCATTTCA	19

In Vitro Functional Analysis

KSP^+ and KSP^- sorted cells fractions, undifferentiated GPSCs, and primary renal tubules were plated on 24-transwell (polycarbonate membrane; Corning). TEER analysis was performed 7 days after cells plating using an STX2 electrode (EVOM2; World Precision Instruments, Inc.); this allowed the formation of tight junction. Electrical resistance can be derived continuously and measured with an ohmmeter. TEER values were expressed in ohm × cm^2.

Production of Biotinylated Probe for *In Situ* Analysis of Y Chromosome

The probe was synthesized starting from a bacterial artificial chromosome (RP24–418C24; Children's Hospital Oakland Research Institute) that cover a specific telomeric region of Y chromosome, the *RBMY* gene. A biotinylated probe was produced by using the random priming method to insert biotinylated deoxyuridine triphosphates (dUTPs) (BioPrime DNA Labeling System; Invitrogen). Probes were purified by passing through purification columns (Illustra Microspin G-50 Columns; GE Healthcare Life Science). *In situ* analysis was performed on paraffin-embedded sections (3.5 μm). Antigens were retrieved using a SPOT-Light Tissue Pretreatment kit (Invitrogen). Sections were denatured at 70°C for 5 minutes and then hybridized at 37°C for 19 hours. The biotinylated dUTPs were revealed with Cy3-conjugated streptavidin (Jackson ImmunoResearch Laboratories, Inc.). We scored the percentage of cells capable of kidney homing by counting 10 sections 10 μm apart. The number of Y^+ chromosomes was calculated on the total number of nuclei.

Animal Model

Studies were conducted in accordance with National Institutes of Health Guide for Care and Use of Laboratory Animals. All experiments were performed with 8-week-old female 129sv/C57; mice were allowed free access to water and standard mouse chow. Renal IRI was

Downloaded from http://journals.lww.com/jasn by BhDMf5ePHKav1zEoum1tQfN4a+kJLhEZgbsIHo4XMi0hCywCX1AWnYQp/IlQrHD3i3D0OdRyi7TvSFl4Cf3VC1y0abggQZXdgGj2MwlZLeI= on 06/10/2024

modified from methods previously described.[57,58] In brief, mice were anesthetized by intraperitoneal injection with Zoletil 100 (Virbac), 2 mg/kg body weight. The left renal artery and vein were clamped for 40 minutes with a nontraumatic microaneurysm clamp, and right nephrectomy was performed. During the period of ischemia, body temperature was maintained at 37°C by placing the mice on a warming pad. After clamp removal, reperfusion was confirmed by visual inspection. To test the effect of GTCs, mice were divided in two groups. In the treated group (n=8), soon after IRI, 2.5×10^5 GTCs, at day 35 of differentiation, were infused intravenously through the tail vein. In the untreated group (n=8), mice were given only vehicle. Both groups were euthanized 2 days after IRI. In the chronic damage model, the same experimental procedure was performed but mice (n=10 treated/untreated group) were euthanized 6 weeks after ischemia.

Identification of CFSE-Labeled Cells

To detect GTCs in renal parenchyma, cells were labeled before injection with CFSE. The cells were injected after IRI in mice tails. Two days after injection, mice were euthanized and kidneys were embedded in optimal cutting temperature compound (VWR DBH Prolabo) and snap-frozen in liquid nitrogen. Tissue slides were stained with an anti-fluorescein/Oregon green polyclonal antibody (Molecular Probes) to detect CFSE-positive cells. DAPI (Sigma-Aldrich) was used to stain nuclei.

Renal Morphology and Tubular Dilation/Cystic Index

For all histologic analyses, kidneys were fixed overnight in 10% formalin and then embedded in paraffin. Renal histology was evaluated by staining kidney sections with periodic acid-Schiff reagents according to the manufacturer's instructions (Bio-Optica). Luminal hyaline CAST and tubular necrosis were assessed in 20 nonoverlapping fields using a 20× objective (Olympus BH2 RFCA). For tubular dilation/cyst formation, sections were stained with hematoxylin and eosin (Bio-Optica). Numbers of CAST and tubular profiles showing necrosis were recorded in a blinded fashion. Tubular dilation/cyst quantification was performed using a screen with dots distant one from another by 13.625 microns. The degree of tubular dilation was defined by the number of dots in the lumen, following previously suggested criteria.[59]

In the chronic damage experiment, kidney sections (3.5 μm) were stained with picrosirius red (Sigma-Aldrich) to assess the amount of fibrosis.[60] The quantification of fibrosis extension was evaluated with MetaMorph software (Molecular Devices, LLC); results were expressed as the mean ratio of the stained area to the total tissue area. Glomerular sclerosis was defined as the presence of dense abundant deposition of periodic acid Schiff–positive material at the glomerular tuft, with occlusion of capillary loops and segmental hyalinization in 100 consecutive glomeruli, by determining the percentage of glomeruli exhibiting sclerotic lesion. Masson trichrome (Bio-Optica) staining was performed according to manufacturer's instruction to evaluate tubular atrophy and interstitial fibrosis. The number of atrophic tubules were evaluated in 10 nonoverlapping fields using a 20× objective (Olympus BH2 RFCA). The quantification of fibrosis was evaluated as the extension of fibrotic area to the total tissue area with MetaMorph software. The scoring of CKD was carried out by a blinded observer through a semiquantitative evaluation, based on arbitrary score on Masson trichrome sections. The score ranged from 0 to 3+ as follows 0: no changes; 1+: damage to <25% of the interstitial area; 2+: damage to 25%–50% of the interstitial area; and 3+: damage to >50% of the interstitial area. Kidney and mice were weighed 6 weeks after ischemia; the relative percentage of kidney weight was evaluated on the weight of mice total body.

In Vivo Apoptosis, Proliferation, Cell Infiltration, and HO-1 Expression

To determine the degree of infiltrating cells and HO-1 expression, renal sections of 3.5 μm were analyzed. Anti-CD18 antibody (BMA Biomedicals; clone YTS 213.1) was used as a marker of inflammatory infiltrates, and anti-HO-1 antibody (Enzo Life Sciences) was used to evaluate the level of HO-1 expression.

To evaluate the proliferation rate, mice were injected intraperitoneally with BrdU (BD Pharmigen), 100 mg/kg body weight, 24 hours after IRI (or 24 hours before euthanasia in the case of CKD) and 50 mg/kg body weight 36 hours after IRI (12 hours before euthanasia for CKD experiment).[61] Kidney sections were deparaffinized and boiled for 15 minutes in 6 mM sodium citrate buffer (pH, 6.0) for HO-1 and BrdU staining (DAKO; clone Bu20a). Antigen retrieval for CD18 staining was accomplished through digestion with 0.005% trypsin for 30 minutes. Nonspecific binding and endogenous peroxidase activity were blocked using 3% hydrogen peroxidase.

Apoptosis was measured by terminal deoxynucleotidyl transferase–mediated dUTP nick-end labeling performed on paraffin-embedded tissue sections using the fluorescein-based In Situ Cell Death Detection kit (Roche) according to the manufacturer's instruction. $BrdU^+$ and $CD18^+$ cells were scored by counting the number of positive cells per field in 20 randomly chosen sections of kidney cortex using a 20× objective (Olympus BH2 RFCA). $TUNEL^+$ cells were scored in 10 randomly chosen sections of kidney using 40× objective (ApoTome, Zeiss). The number of $BrdU^+$ cells and $TUNEL^+$ cells was normalized on the number of total nuclei.

Renal Functionality Assessment

To assess renal functionality, serum was collected. Blood samples were incubated at 37°C for 30 minutes to allow blood clotting. Serum was then isolated from the supernatant by centrifugation of blood samples (3000 rpm, 10 minutes). Creatinine level was measured using a colorimetric assay based on the Jaffe reaction (Quantichrom Creatinine Assay; BioAssay Systems, Hayward, CA). BUN was measured by direct quantification of serum urea with a colorimetric assay kit according to the instruction protocol (Quantichrom Urea Assay; BioAssay Systems).

Cystatin C level was assayed by ELISA according to the manufacturer's instruction (Abcam).

Teratoma Formation Assay

To assess teratoma formation, after 42 days of differentiation in culture, GTCs were injected under renal capsule. A total of 1×10^6 GTCs or undifferentiated GPSCs, both from two independent cultures, were resuspended in 100 μl of PBS. The 129sv/C57 mice were anesthetized by an intraperitoneal injection with zoletil 100 (Virbac), 2 mg/kg body weight, and cell suspensions were injected under the left renal capsule. Mice were euthanized after 6 weeks, and the left kidneys were removed to check teratoma formation. Right

kidneys were used as positive controls. Kidney sections (3.5 μm) were stained with hematoxylin and eosin to analyze teratoma composition.

Statistical Analyses

Values were reported as the mean ± SEM. Statistical analyses were performed by using the two-tailed t test ($^{*}P<0.05$; $^{**}P<0.01$; $^{***}P<0.001$) for the graphs comparing only two variables. For analysis of more than two categories, statistical significance was calculated with one-way ANOVA and Bonferroni post-tests ($^{*}P<0.05$; $^{**}P<0.01$; $^{***}P<0.001$). All analyses were performed with PRISM5 (GraphPad Software, Inc., La Jolla, CA).

Downloaded from http://journals.lww.com/jasn by BhDMf5ePHKav1zEoum1tQfN4a+kJLhEZgbsIHo4XMi0hCywCX1AWnYQp/IlQrHD3i3D0OdRyi7TvSFl4Cf3VC1y0abggQZXdgGj2MwlZLeI= on 06/10/2024

ACKNOWLEDGMENTS

This work was supported by the following grants to F.A.: Piattaforma Regione Piemonte Pi-Stem and PRIN 2010-2012. We thank Gabriele Bonifacio and Lucia Damicis for help with experiments and Flavio Cristofani, Ornella Azzolino, and Antonellisa Sgarra for helping in mouse breeding and animal care work.

DISCLOSURES

None.

REFERENCES

1. Bonventre JV, Yang L: Cellular pathophysiology of ischemic acute kidney injury. *J Clin Invest* 121: 4210–4221, 2011
2. Eltzschig HK, Eckle T: Ischemia and reperfusion—from mechanism to translation. *Nat Med* 17: 1391–1401, 2011
3. Takahashi K, Yamanaka S: Induction of pluripotent stem cells from mouse embryonic and adult fibroblast cultures by defined factors. *Cell* 126: 663–676, 2006
4. Stadtfeld M, Apostolou E, Akutsu H, Fukuda A, Follett P, Natesan S, Kono T, Shioda T, Hochedlinger K: Aberrant silencing of imprinted genes on chromosome 12qF1 in mouse induced pluripotent stem cells. *Nature* 465: 175–181, 2010
5. Lister R, Pelizzola M, Kida YS, Hawkins RD, Nery JR, Hon G, Antosiewicz-Bourget J, O'Malley R, Castanon R, Klugman S, Downes M, Yu R, Stewart R, Ren B, Thomson JA, Evans RM, Ecker JR: Hotspots of aberrant epigenomic reprogramming in human induced pluripotent stem cells. *Nature* 471: 68–73, 2011
6. Kanatsu-Shinohara M, Inoue K, Ogonuki N, Morimoto H, Ogura A, Shinohara T: Serum- and feeder-free culture of mouse germline stem cells. *Biol Reprod* 84: 97–105, 2011
7. Sato T, Katagiri K, Gohbara A, Inoue K, Ogonuki N, Ogura A, Kubota Y, Ogawa T: In vitro production of functional sperm in cultured neonatal mouse testes. *Nature* 471: 504–507, 2011
8. Kanatsu-Shinohara M, Inoue K, Lee J, Yoshimoto M, Ogonuki N, Miki H, Baba S, Kato T, Kazuki Y, Toyokuni S, Toyoshima M, Niwa O, Oshimura M, Heike T, Nakahata T, Ishino F, Ogura A, Shinohara T: Generation of pluripotent stem cells from neonatal mouse testis. *Cell* 119: 1001–1012, 2004
9. Guan K, Nayernia K, Maier LS, Wagner S, Dressel R, Lee JH, Nolte J, Wolf F, Li M, Engel W, Hasenfuss G: Pluripotency of spermatogonial stem cells from adult mouse testis. *Nature* 440: 1199–1203, 2006
10. Seandel M, James D, Shmelkov SV, Falciatori I, Kim J, Chavala S, Scherr DS, Zhang F, Torres R, Gale NW, Yancopoulos GD, Murphy A, Valenzuela DM, Hobbs RM, Pandolfi PP, Rafii S: Generation of functional multipotent adult stem cells from GPR125+ germline progenitors. *Nature* 449: 346–350, 2007
11. Ko K, Tapia N, Wu G, Kim JB, Bravo MJ, Sasse P, Glaser T, Ruau D, Han DW, Greber B, Hausdörfer K, Sebastiano V, Stehling M, Fleischmann BK, Brüstle O, Zenke M, Schöler HR: Induction of pluripotency in adult unipotent germline stem cells. *Cell Stem Cell* 5: 87–96, 2009
12. Guan K, Wagner S, Unsöld B, Maier LS, Kaiser D, Hemmerlein B, Nayernia K, Engel W, Hasenfuss G: Generation of functional cardiomyocytes from adult mouse spermatogonial stem cells. *Circ Res* 100: 1615–1625, 2007
13. Streckfuss-Bömeke K, Vlasov A, Hülsmann S, Yin D, Nayernia K, Engel W, Hasenfuss G, Guan K: Generation of functional neurons and glia from multipotent adult mouse germ-line stem cells. *Stem Cell Res (Amst)* 2: 139–154, 2009
14. Yoshimoto M, Heike T, Chang H, Kanatsu-Shinohara M, Baba S, Varnau JT, Shinohara T, Yoder MC, Nakahata T: Bone marrow engraftment but limited expansion of hematopoietic cells from multipotent germline stem cells derived from neonatal mouse testis. *Exp Hematol* 37: 1400–1410, 2009
15. Fagoonee S, Hobbs RM, De Chiara L, Cantarella D, Piro RM, Tolosano E, Medico E, Provero P, Pandolfi PP, Silengo L, Altruda F: Generation of functional hepatocytes from mouse germ line cell-derived pluripotent stem cells in vitro. *Stem Cells Dev* 19: 1183–1194, 2010
16. Im JE, Song SH, Kim JY, Kim KL, Baek SH, Lee DR, Suh W: Vascular differentiation of multipotent spermatogonial stem cells derived from neonatal mouse testis. *Exp Mol Med* 44: 303–309, 2012
17. Wu DP, He DL, Li X, Liu ZH: Differentiations of transplanted mouse spermatogonial stem cells in the adult mouse renal parenchyma in vivo. *Acta Pharmacol Sin* 29: 1029–1034, 2008
18. Kobayashi T, Tanaka H, Kuwana H, Inoshita S, Teraoka H, Sasaki S, Terada Y: Wnt4-transformed mouse embryonic stem cells differentiate into renal tubular cells. *Biochem Biophys Res Commun* 336: 585–595, 2005
19. Kim D, Dressler GR: Nephrogenic factors promote differentiation of mouse embryonic stem cells into renal epithelia. *J Am Soc Nephrol* 16: 3527–3534, 2005
20. Bruce SJ, Rea RW, Steptoe AL, Busslinger M, Bertram JF, Perkins AC: In vitro differentiation of murine embryonic stem cells toward a renal lineage. *Differentiation* 75: 337–349, 2007
21. Vigneau C, Polgar K, Striker G, Elliott J, Hyink D, Weber O, Fehling HJ, Keller G, Burrow C, Wilson P: Mouse embryonic stem cell-derived embryoid bodies generate progenitors that integrate long term into renal proximal tubules in vivo. *J Am Soc Nephrol* 18: 1709–1720, 2007
22. Morizane R, Monkawa T, Itoh H: Differentiation of murine embryonic stem and induced pluripotent stem cells to renal lineage in vitro. *Biochem Biophys Res Commun* 390: 1334–1339, 2009
23. Ren X, Zhang J, Gong X, Niu X, Zhang X, Chen P, Zhang X: Differentiation of murine embryonic stem cells toward renal lineages by conditioned medium from ureteric bud cells in vitro. *Acta Biochim Biophys Sin (Shanghai)* 42: 464–471, 2010
24. Singaravelu K, Padanilam BJ: In vitro differentiation of MSC into cells with a renal tubular epithelial-like phenotype. *Ren Fail* 31: 492–502, 2009
25. Shao X, Johnson JE, Richardson JA, Hiesberger T, Igarashi P: A minimal Ksp-cadherin promoter linked to a green fluorescent protein reporter gene exhibits tissue-specific expression in the developing kidney and genitourinary tract. *J Am Soc Nephrol* 13: 1824–1836, 2002
26. Taub M, Wang Y, Szczesny TM, Kleinman HK: Epidermal growth factor or transforming growth factor alpha is required for kidney tubulogenesis in matrigel cultures in serum-free medium. *Proc Natl Acad Sci U S A* 87: 4002–4006, 1990
27. Cereijido M, Robbins ES, Dolan WJ, Rotunno CA, Sabatini DD: Polarized monolayers formed by epithelial cells on a permeable and translucent support. *J Cell Biol* 77: 853–880, 1978

Downloaded from http://journals.lww.com/jasn by BhDMf5ePHKav1zEoum1tQfN4a+kJLhEZgbsIHo4XMi0hCywCX1AWnYQp/IlQrHD3i3D0OdRyi7TvSFl4Cf3VC1y0abggQZXdgGj2MwlZLeI= on 06/10/2024

28. Ferrell N, Desai RR, Fleischman AJ, Roy S, Humes HD, Fissell WH: A microfluidic bioreactor with integrated transepithelial electrical resistance (TEER) measurement electrodes for evaluation of renal epithelial cells. *Biotechnol Bioeng* 107: 707–716, 2010
29. Liu M, Yang X, Fan J, Zhang R, Wu J, Zeng Y, Nie J, Yu X: Altered tight junctions and fence function in NRK-52E cells induced by aristolochic acid. *Hum Exp Toxicol* 31: 32–41, 2012
30. Dressel R, Guan K, Nolte J, Elsner L, Monecke S, Nayernia K, Hasenfuss G, Engel W: Multipotent adult germ-line stem cells, like other pluripotent stem cells, can be killed by cytotoxic T lymphocytes despite low expression of major histocompatibility complex class I molecules. *Biol Direct* 4: 31, 2009
31. Olszanecki R, Rezzani R, Omura S, Stec DE, Rodella L, Botros FT, Goodman AI, Drummond G, Abraham NG: Genetic suppression of HO-1 exacerbates renal damage: Reversed by an increase in the antiapoptotic signaling pathway. *Am J Physiol Renal Physiol* 292: F148–F157, 2007
32. Zager RA, Johnson AC, Becker K: Acute unilateral ischemic renal injury induces progressive renal inflammation, lipid accumulation, histone modification, and "end-stage" kidney disease. *Am J Physiol Renal Physiol* 301: F1334–F1345, 2011
33. Leung KC, Tonelli M, James MT: Chronic kidney disease following acute kidney injury-risk and outcomes. *Nat Rev Nephrol* 9: 77–85, 2013
34. Benipal B, Lash LH: Influence of renal compensatory hypertrophy on mitochondrial energetics and redox status. *Biochem Pharmacol* 81: 295–303, 2011
35. Feitoza CQ, Gonçalves GM, Semedo P, Cenedeze MA, Pinheiro HS, Beraldo FC, dos Santos OF, Teixeira VP, dos Reis MA, Mazzali M, Pacheco-Silva A, Câmara NO: Inhibition of COX 1 and 2 prior to renal ischemia/reperfusion injury decreases the development of fibrosis. *Mol Med* 14: 724–730, 2008
36. Ko GJ, Boo CS, Jo SK, Cho WY, Kim HK: Macrophages contribute to the development of renal fibrosis following ischaemia/reperfusion-induced acute kidney injury. *Nephrol Dial Transplant* 23: 842–852, 2008
37. Eddy AA, Lopez-Guisa JM, Okamura DM, Yamaguchi I: Investigating mechanisms of chronic kidney disease in mouse models. *Pediatr Nephrol* 27: 1233–1247, 2012
38. Segers VF, Lee RT: Stem-cell therapy for cardiac disease. *Nature* 451: 937–942, 2008
39. Hauser PV, De Fazio R, Bruno S, Sdei S, Grange C, Bussolati B, Benedetto C, Camussi G: Stem cells derived from human amniotic fluid contribute to acute kidney injury recovery. *Am J Pathol* 177: 2011–2021, 2010
40. Jadasz JJ, Aigner L, Rivera FJ, Küry P: The remyelination Philosopher's Stone: Stem and progenitor cell therapies for multiple sclerosis. *Cell Tissue Res* 349: 331–347, 2012
41. Conrad S, Renninger M, Hennenlotter J, Wiesner T, Just L, Bonin M, Aicher W, Bühring HJ, Mattheus U, Mack A, Wagner HJ, Minger S, Matzkies M, Reppel M, Hescheler J, Sievert KD, Stenzl A, Skutella T: Generation of pluripotent stem cells from adult human testis. *Nature* 456: 344–349, 2008
42. Payne CJ, Braun RE: Human adult testis-derived pluripotent stem cells: Revealing plasticity from the germline. *Cell Stem Cell* 3: 471–472, 2008
43. Golestaneh N, Kokkinaki M, Pant D, Jiang J, DeStefano D, Fernandez-Bueno C, Rone JD, Haddad BR, Gallicano GI, Dym M: Pluripotent stem cells derived from adult human testes. *Stem Cells Dev* 18: 1115–1126, 2009
44. Kossack N, Meneses J, Shefi S, Nguyen HN, Chavez S, Nicholas C, Gromoll J, Turek PJ, Reijo-Pera RA: Isolation and characterization of pluripotent human spermatogonial stem cell-derived cells. *Stem Cells* 27: 138–149, 2009
45. Thomson RB, Igarashi P, Biemesderfer D, Kim R, Abu-Alfa A, Soleimani M, Aronson PS: Isolation and cDNA cloning of Ksp-cadherin, a novel kidney-specific member of the cadherin multigene family. *J Biol Chem* 270: 17594–17601, 1995
46. Bonventre JV: Dedifferentiation and proliferation of surviving epithelial cells in acute renal failure. *J Am Soc Nephrol* 14[Suppl 1]: S55–S61, 2003
47. Basile DP, Donohoe DL, Roethe K, Mattson DL: Chronic renal hypoxia after acute ischemic injury: Effects of L-arginine on hypoxia and secondary damage. *Am J Physiol Renal Physiol* 284: F338–F348, 2003
48. Vallabhaneni R, Kaczorowski DJ, Yaakovian MD, Rao J, Zuckerbraun BS: Heme oxygenase 1 protects against hepatic hypoxia and injury from hemorrhage via regulation of cellular respiration. *Shock* 33: 274–281, 2010
49. Shiraishi F, Curtis LM, Truong L, Poss K, Visner GA, Madsen K, Nick HS, Agarwal A: Heme oxygenase-1 gene ablation or expression modulates cisplatin-induced renal tubular apoptosis. *Am J Physiol Renal Physiol* 278: F726–F736, 2000
50. Pittock ST, Norby SM, Grande JP, Croatt AJ, Bren GD, Badley AD, Caplice NM, Griffin MD, Nath KA: MCP-1 is up-regulated in unstressed and stressed HO-1 knockout mice: Pathophysiologic correlates. *Kidney Int* 68: 611–622, 2005
51. Ferenbach DA, Ramdas V, Spencer N, Marson L, Anegon I, Hughes J, Kluth DC: Macrophages expressing heme oxygenase-1 improve renal function in ischemia/reperfusion injury. *Mol Ther* 18: 1706–1713, 2010
52. Ferenbach DA, Nkejabega NC, McKay J, Choudhary AK, Vernon MA, Beesley MF, Clay S, Conway BC, Marson LP, Kluth DC, Hughes J: The induction of macrophage hemeoxygenase-1 is protective during acute kidney injury in aging mice. *Kidney Int* 79: 966–976, 2011
53. Hirashima M, Ogawa M, Nishikawa S, Matsumura K, Kawasaki K, Shibuya M, Nishikawa S: A chemically defined culture of VEGFR2+ cells derived from embryonic stem cells reveals the role of VEGFR1 in tuning the threshold for VEGF in developing endothelial cells. *Blood* 101: 2261–2267, 2003
54. Gupta S, Verfaillie C, Chmielewski D, Kren S, Eidman K, Connaire J, Heremans Y, Lund T, Blackstad M, Jiang Y, Luttun A, Rosenberg ME: Isolation and characterization of kidney-derived stem cells. *J Am Soc Nephrol* 17: 3028–3040, 2006
55. Morais C, Westhuyzen J, Pat B, Gobe G, Healy H: High ambient glucose is effect neutral on cell death and proliferation in human proximal tubular epithelial cells. *Am J Physiol Renal Physiol* 289: F401–F409, 2005
56. Terryn S, Jouret F, Vandenabeele F, Smolders I, Moreels M, Devuyst O, Steels P, Van Kerkhove E: A primary culture of mouse proximal tubular cells, established on collagen-coated membranes. *Am J Physiol Renal Physiol* 293: F476–F485, 2007
57. Park KM, Chen A, Bonventre JV: Prevention of kidney ischemia/reperfusion-induced functional injury and JNK, p38, and MAPK kinase activation by remote ischemic pretreatment. *J Biol Chem* 276: 11870–11876, 2001
58. Gatti S, Bruno S, Deregibus MC, Sordi A, Cantaluppi V, Tetta C, Camussi G: Microvesicles derived from human adult mesenchymal stem cells protect against ischaemia-reperfusion-induced acute and chronic kidney injury. *Nephrol Dial Transplant* 26: 1474–1483, 2011
59. Bastos AP, Piontek K, Silva AM, Martini D, Menezes LF, Fonseca JM, Fonseca II, Germino GG, Onuchic LF: Pkd1 haploinsufficiency increases renal damage and induces microcyst formation following ischemia/reperfusion. *J Am Soc Nephrol* 20: 2389–2402, 2009
60. Semedo P, Donizetti-Oliveira C, Burgos-Silva M, Cenedeze MA, Avancini Costa Malheiros DM, Pacheco-Silva A, Câmara NO: Bone marrow mononuclear cells attenuate fibrosis development after severe acute kidney injury. *Lab Invest* 90: 685–695, 2010
61. deFazio A, Leary JA, Hedley DW, Tattersall MH: Immunohistochemical detection of proliferating cells in vivo. *J Histochem Cytochem* 35: 571–577, 1987

This article contains supplemental material online at http://jasn.asnjournals.org/lookup/suppl/doi:10.1681/ASN.2013040367/-/DCSupplemental.